



Quercetin mediated antimicrobial photodynamic treatment using blue light on *Escherichia coli* O157:H7 and *Listeria monocytogenes*

In-Hwan Lee^{a,1}, Soo-Hwan Kim^{a,1}, Dong-Hyun Kang^{a,b,*}

^a Department of Agricultural Biotechnology, Center of Food and Bioconvergence, Research Institute of Agriculture and Life Sciences, Seoul National University, Seoul, 08826, Republic of Korea

^b Institutes of Green Bio Science and Technology, Seoul National University, Pyeong-Chang, Gangwon-do, 25354, Republic of Korea

ARTICLE INFO

Handling Editor: Siyun Wang

Keywords:

Quercetin
Photodynamic treatment
Reactive oxygen species
405 nm blue Light
Foodborne pathogens

ABSTRACT

Interest in using an antimicrobial photodynamic treatment (aPDT) for the microbial decontamination of food has been growing. In this study, quercetin, a substance found ubiquitously in plants, was used as a novel exogenous photosensitizer with 405 nm blue light (BL) for the aPDT on foodborne pathogens, and the inactivation mechanism was elucidated. The inactivation of *Escherichia coli* O157:H7 and *Listeria monocytogenes* in PBS solution by the quercetin and BL combination treatment reached a log reduction of 6.2 and more than 7.55 at 80 J/cm² (68 min 21 s), respectively. When EDTA was added to investigate the reason for different resistance between two bacteria, the effect of aPDT was enhanced against *E. coli* O157:H7 but not *L. monocytogenes*. This result indicated that the lipopolysaccharide of Gram-negative bacteria operated as a protective barrier. It was experimentally demonstrated that quercetin generated the superoxide anion and hydrogen peroxide as the reactive oxygen species that oxidize and inactivate cell components. The damage to the bacterial cell membrane by aPDT was evaluated by propidium iodide, where the membrane integrity significantly ($P < 0.05$) decreased from 40 J/cm² compared to control. In addition, DNA integrity of bacteria was significantly ($P < 0.05$) more decreased after aPDT than BL treatment. The inactivation results could be applied in liquid food industries for decontamination of foodborne pathogens, and the mechanisms data was potentially utilized for further studies about aPDT using quercetin.

1. Introduction

Consumer concern about contamination of food by microorganisms has grown for health reasons (Sheng and Zhu, 2021). However, foodborne outbreak related with liquid food such as milk and fruit juice has constantly reported, causing the hospitalization and death of people every year (Mostafidi et al., 2020; Sebastianski et al., 2022). Among these outbreak, *Escherichia coli* O157:H7 and *Listeria monocytogenes*, were strongly associated with milk and fruit juice contamination, and recently 12 patients and one died due to *L. monocytogenes* in cheese made by pasteurized milk in 2021 (Palacios et al., 2022; Treacy et al., 2019). It is well-known that *E. coli* O157:H7 can produce Shiga-like toxins that cause hemorrhagic colitis and hemolytic uremic syndrome (Kolodziejek et al., 2022), and *L. monocytogenes* produces listeriolysin O to escape host macrophages and caused listeriosis, which was especially fatal to expectant mothers (Pal et al., 2022). Therefore, it is of great

importance to inactivate these pathogens in liquid food, especially in milk and fruit juice. However, despite the use of representative microbial decontamination strategies such as ultraviolet (UV) treatment and heat treatment, some problems were remaining such as low penetration of UV-C (Delorme et al., 2020) or protein denaturation by heating (Liu et al., 2020).

For beverage pasteurization, antimicrobial photodynamic treatment (aPDT) is an alternative technology that produces multitargeting reactive oxygen species (ROS), which were proved to attenuate virulence factors and oxidize macromolecules such as lipopolysaccharide, leading to disruption of cell structure (Sheng et al., 2022). In general, light source, type of photosensitizer, and oxygen are essential components in PDI (M.-Y. Park and Kang, 2021). When it comes to the safety for workers, the advantage of aPDT is that it uses the visible light region with natural compounds such as chlorophyll, curcumin, and riboflavin. Therefore, it can be more harmless to the human body than UV-C and

* Corresponding author. Department of Agricultural Biotechnology, Seoul National University, Seoul, Republic of Korea.

E-mail address: kang7820@snu.ac.kr (D.-H. Kang).

¹ In-Hwan Lee and Soo-Hwan Kim contributed equally to this work.

<https://doi.org/10.1016/j.crf.2022.100428>

Received 25 July 2022; Received in revised form 20 December 2022; Accepted 22 December 2022

Available online 30 December 2022

2665-9271/© 2022 Published by Elsevier B.V. This is an open access article under the CC BY-NC-ND license (<http://creativecommons.org/licenses/by-nc-nd/4.0/>).

chlorine-based sanitizer (Brovko, 2010; Lui et al., 2016). The production processes of ROS are three steps of the transmission of energy from light to photosensitizer (PSs), intersystem crossing (ISC) of excited PSs, and the transference of energy from PSs to oxygen and water (Ghate et al., 2019). Reactions with PSs can be classified as type I or type II (Dias et al., 2020). In a type I reaction, a photosensitizer is disassembled by transferring high energy electrons to substrates, resulting in the production of ROS, such as hydrogen peroxide (H_2O_2) and the superoxide anion ($O_2^{\cdot -}$). In a type II reaction, PSs transfer energy from a light source to oxygen to produce singlet oxygen (1O_2). Although the two different types of reaction type can occur simultaneously, the main reaction is determined by the PSs involved and the aPDT environment (Silva et al., 2018).

PSs can be classified as endogenous or exogenous (Ghate et al., 2019). Endogenous PSs exist in bacterial cells (Lukšienė and Zukauskas, 2009). A porphyrin is a representative endogenous photosensitizer with an absorption wavelength of 400–430 nm (Amin et al., 2016). Contrary to endogenous PSs, exogenous PSs are additional compound to enhance antimicrobial effect of aPDT. Exogenous PSs contain natural compounds from plants and synthetic compounds (Hamblin, 2016). The application of numerous available PSs is restricted from being used in foods for safety reasons. Therefore, only a few natural PSs can be applied against pathogenic bacteria for food safety. To illustrate, curcumin is a PS that has been actively studied for use in aPDT applied to food. *E. coli* O157:H7 and *Listeria innocua* populations in aqueous solution were decreased more than 4 or 5 log reduction, respectively, after 15 min of treatment with curcumin and UV-A light (320–400 nm) or curcumin and visible light (400–800 nm) (de Oliveira et al., 2018).

Quercetin is a natural flavonoid compound that is ubiquitous in plants, especially fruits and vegetables (Boots et al., 2008). Quercetin has many biological activities, such as anticancer, anti-inflammatory, and antioxidant activities, that can improve human health (Lesjak et al., 2018; Priya et al., 2014). Thus, quercetin supplements of less than 500 mg were added to the generally recognized as safe (GRAS) list of the Food and Drug Administration in 2010 (Y.-M. Zhang et al., 2020). Quercetin has the potential to be used as a photosensitizer due to absorbing light range from UV-A to visible light (Sengupta and Sengupta, 2002). In the previous study, the potential photosensitization effect of quercetin was evaluated. A study showed that *S. aureus* counts on film were effectively reduced (>6 log) by aPDT using quercetin and visible light, but there was no reduction in *E. coli* counts (Condat et al., 2016).

To the best of our knowledge, no studies have been conducted on the inactivation of foodborne pathogens by a quercetin and BL. Therefore, the objective of this study was to determine the potential of quercetin as a natural photosensitizer for food safety by analyzing the antimicrobial effect of a quercetin and BL combination treatment, the resistance of Gram-negative and Gram-positive bacterium against aPDT, the ROS produced in solution, and the inactivation mechanism.

2. Materials and methods

2.1. Preparation of bacterial culture and suspension

The *E. coli* O157:H7 (ATCC 35150, ATCC 43889, ATCC 43890) and *L. monocytogenes* (ATCC 15313, ATCC 19111, ATCC 19115) used in this study were acquired from the bacterial culture collection of the Center for Food Science, Seoul National University (Seoul, South Korea). Each strain was preserved in 0.7 ml of tryptic soy broth (TSB) (MBCell, Seocho-Gu, Seoul, South Korea) and 0.3 ml of 50% glycerol at -80°C . Working cultures were prepared by streaking onto tryptic soy agar (TSA) (MBCell, Seocho-Gu, Seoul, South Korea), followed by incubation at 37°C for 24 h, and storage at 4°C . A single colony of each strain was cultivated in 5 ml of TSB at 37°C for 20–24 h with shaking at 250 rpm. Incubated cells were mixed and centrifuged ($4000\times g$) at 4°C for 20 min to harvest cell pellet. The cell pellet resuspended in 9 ml of phosphate-buffered saline (PBS; pH 7.4; Corning, Manassas, USA) to obtain a bacterial culture cocktail at a

final concentration of approximately 10^9 – 10^{10} CFU/ml.

2.2. Preparation of quercetin solution

The quercetin used in this study ($\geq 95\%$ HPLC (purity), solid) (Sigma-Aldrich, St. Louis, USA) was purchased, and liquid food samples (milk and white grape juice were purchased at local grocery store. Preparation of a stock solutions referred to preparation of another photosensitizer (Nima et al., 2021). A stock solution was prepared by dissolving 3.75 mM quercetin in ethanol, followed by filtering through a 0.22 μm syringe filter. The stock solution was diluted to appropriate concentration in 10 ml PBS solution (50, 75, or 100 μM), milk (75 μM), and white grape juice (75 μM) in a 60×15 mm petri dish for aPDT.

2.3. Light source

A 405 nm blue light emitting diode (LED) with a radiant flux of 10 mW was used as the light source. Three LEDs were used with an aluminum heat sink to prevent heat effects. The emission spectra were measured by a spectrometer (AvaSpec-ULS2048-USB2-UA-50; Avantes, Apeldoorn, Netherlands). The LED had a full width at half maximum (FWHM) of 16.15 nm.

2.4. Inoculation of bacterial suspension and aPDT

The sample was prepared for treatment by inoculating 50 μl aliquots of the bacterial suspension in 10 ml quercetin solution (PBS, milk, and white grape juice) in a 60×15 mm petri dish. The LED was placed 4.5 cm from the bottom of the petri dish. The light dose was determined by estimating the intensity using the petri factor as described in previous study (Kim et al., 2020). The irradiance value was measured at 10 points spaced 1 cm apart in a 60×15 mm petri dish, and the petri factor was calculated as the average proportion of the maximum irradiance value at each point. The intensity value was obtained by multiplying petri factor and the maximum irradiation value to calculate the treatment time when the dose value of LEDs was 20, 40, 60, 80, and 120 J/cm^2 . The intensity value was 19.5 mW/cm^2 for LEDs and the treatment time was 17 min 4 s, 34 min 8 s, 51 min 17 s, 68 min 21 s, and 102 min 30 s for 20, 40, 60, 80, and 120 J/cm^2 . Sequential dose from 20 to 80 J/cm^2 were irradiated for PBS disinfection, and different dose of 40 and 80 J/cm^2 (*E. coli* O157:H7) or 80 and 120 J/cm^2 (*L. monocytogenes*) were irradiated for milk, while that of 20 and 40 J/cm^2 were irradiated for white grape juice, respectively. The treatment sample in the petri dish was placed below the center of three LEDs, gently agitated with an 8 mm magnetic bar, and illuminated at the prescribed dose at room temperature. The sample depth from the bottom of petri dish was 0.5 cm. Samples without illumination or quercetin treatment were also evaluated to clarify the effect of aPDT.

2.5. Combination with EDTA

EDTA test was conducted following a previous study with some modifications (Hu et al., 2018). One of the different factors between Gram-negative and Gram-positive bacteria is existence of lipopolysaccharides (LPS). To elucidate the function of LPS, ethylenediaminetetraacetic acid disodium salt dihydrate (EDTA-2Na) (Junsei, Tokyo, Japan) was used. For aPDT, 10 ml of quercetin (75 μM)-EDTA (1 mM) solution with bacteria was irradiated at the dose of 20, 40, 60, and 80 J/cm^2 at the same treatment setup with inactivation experiments conditions.

2.6. Bacterial enumeration

One milliliter aliquots of the treated or untreated sample were serially diluted 10-fold in 9 ml of 0.2% sterilized peptone water (PW) (Becton, Dickinson and Company, Sparks, MD, USA), and 0.1 ml of the

treated sample or diluent was inoculated and spread onto each selective medium. A volume of 250 μl of the treated sample was directly plated onto each medium if low numbers of surviving cells were anticipated. The selective media used were sorbitol MacConkey agar (SMAC) (Difco, Sparks, MD, USA) for *E. coli* O157:H7 and Oxford agar (MBcell) (Seochogu, Seoul, South Korea) with Oxford agar supplement (MBcell) (Seochogu, Seoul, South Korea) for *L. monocytogenes*. The occurrence of sublethally injured *E. coli* O157:H7 and *L. monocytogenes* in food samples after aPDT was investigated using the broth recovery method (Han et al., 2019). Treated or untreated sample 1 ml was poured into 9 ml of TSB and incubated at 37 °C for 2 h. After incubation, resuscitated pathogens in TSB was serially diluted 10-fold in 9 ml of 0.2% sterilized PW, and 100 μl or 1 ml of the diluent was spread onto SMAC and Oxford agar. All the selective agar media were incubated in dark at 37 °C for 24–48 h, after which the typical colonies were counted. Log reduction values of the pathogens in PBS with different concentration of quercetin or liquid food samples were determined by subtracting the number of colonies counted in the treated sample from the number of colonies counted in control.

2.7. Measurement of ROS ($^1\text{O}_2$, O_2^* , and H_2O_2) without cells

As described above, ROS play an important role in inactivating pathogens in aPDT. Therefore, $^1\text{O}_2$, O_2^* , and H_2O_2 were detected using *N,N*-dimethyl-4-nitrosoaniline (RNO) (Sigma-Aldrich, St. Louis, USA) and imidazole (Sigma-Aldrich, St. Louis, USA); 2,3-bis (2-methoxy-4-nitro-5-sulphonyl)-2H-tetrazolium-5-carboxanilide (XTT) (Thermo Fisher Scientific, Rockford, USA); and glutathione (GSH) (Sigma-Aldrich, St. Louis, USA) and 5,5-dithio-bis-(2-nitrobenzoic acid) (DTNB) (Thermo Fisher Scientific, Rockford, USA), respectively (Y. Zhang et al., 2018). Stock solutions of 0.5 mM RNO, 80 mM imidazole, 1 mM XTT, 10 mM GSH, and 100 mM DTNB were prepared in PBS. The $^1\text{O}_2$ detection experiment was performed using final concentrations of RNO and imidazole of 50 μM and 8 mM, respectively, in 10 ml of PBS solution supplemented with 75 μM quercetin without cells in a 60 \times 15 mm petri dish. The sample was treated with light of from 20 to 80 J/cm^2 under gently stirring, and the absorbance of 0.2 ml aliquots was then measured with a spectrofluorophotometer at a wavelength of 440 nm in a 96-well plate. For O_2^* detection, an XTT stock solution was mixed with PBS solution added with 75 μM quercetin to obtain a final concentration of 0.2 mM without cells. The absorbance of 0.2 ml aliquots of the treated sample at the dose from 20 to 80 J/cm^2 was measured at a wavelength of 470 nm in a 96-well plate. The sample without cells was mixed with a final concentration of 0.1 mM GSH and 10 ml of the PBS solution included with 75 μM quercetin and irradiated at the dose from 20 to 80 J/cm^2 . Ten microliters of DTNB were mixed with 1 ml aliquots of the irradiated sample and analyzed at a wavelength of 412 nm in a 96-well plate. All the experiments were conducted with a negative control that was not subjected to quercetin treatment or illumination.

2.8. Measurement of quercetin uptake

It is important to determine whether quercetin was present inside or outside the cell membrane during ROS production under illumination and quercetin treatment. Hence, the quercetin uptake by bacteria was measured using a diphenyl boric acid-2-aminoethyl ester (DPBA) (Sigma-Aldrich, St. Louis, USA) that amplifies the fluorescence of flavonoids by binding (Buer et al., 2010). A mixture containing 0.2% (w/v in dimethyl sulfoxide (DMSO) (Sigma-Aldrich, St. Louis, USA)) DPBA, 10 ml PBS, quercetin (75 μM) and each bacterial strain was prepared. For the analysis, the cell concentrations of *E. coli* O157:H7 and *L. monocytogenes* were adjusted to an optical density at a wavelength of 600 nm (OD_{600}) of 0.3 in PBS solution. The mixture was treated with BL at 20, 40, 60, and 80 J/cm^2 or incubated in the dark. The treated sample was centrifuged (10,000 \times g, 5 min) and washed twice with PBS to remove the remaining quercetin. The pellet was dissolved in 450 μl of

DPBA, and the fluorescence was measured with a spectrofluorophotometer at excitation and emission wavelengths of 480 and 535 nm. The measured fluorescence was divided by OD_{600} for normalization.

2.9. Assessment of damage to cell membrane and DNA

The antimicrobial mechanism of aPDT was investigated using propidium iodide (PI) (Sigma-Aldrich, St. Louis, USA) and SYBR green I [2-[N-(3-dimethylaminopropyl)-N-propylamino]-4-[2,3-dihydro-3-methyl-(benzo-1,3-thiazol-2-yl)-methylidene]-1-phenylquinolinium] (Sigma-Aldrich, St. Louis, USA). PI can penetrate the damaged cell membrane and intercalate to DNA and was therefore used as the fluorescent probe to investigate the permeability of the cell membrane (Stiefel et al., 2015). SYBR green I can emit fluorescence when binding intact double strand DNA (Deprez et al., 2002). Therefore, the integrity of DNA was assessed by the loss rate of the fluorescence after aPDT. For the assessment, the cell concentrations of *E. coli* O157:H7 and *L. monocytogenes* were adjusted to an OD_{600} of 0.3 in PBS with 75 μM quercetin.

To measure membrane damage, 405-nm blue LEDs at light doses of 20, 40, 60, and 80 J/cm^2 , and 75 μM quercetin were used for aPDT. The treated or untreated cells were collected by centrifugation (10,000 \times g, 5 min), and the pellet was resuspended in 1 ml of PBS. The following experiment was conducted using a previously reported method (Cho and Kang, 2022). PI at a final concentration of 2.9 μM was mixed with the resuspended solution and incubated at 37 °C for 10 min. The cells were collected by centrifugation (10,000 \times g) and washed twice with PBS. The pellet was resuspended in 1 ml of PBS, and the fluorescence was measured with a spectrofluorophotometer at excitation and emission wavelengths of 493 and 630 nm. The fluorescence was normalized by OD_{600} and substituted into the following formula:

$$(\text{Fluorescence of treated sample}/\text{OD}_{600}) - (\text{Fluorescence of untreated sample}/\text{OD}_{600})$$

For measurement of DNA damage, each cell was treated by quercetin 75 μM , illumination with BL at 80 J/cm^2 , or quercetin combined with BL treatment at 80 J/cm^2 . After treatment, the cell pellet was collected by centrifugation (10,000 \times g, 5 min). The extracted 100 μl DNA was obtained using a commercial DNA extraction kit (Genelix bead kit; Sanigen Co., Ltd., Anyang, Republic of Korea). SYBR green I solution was added to DNA solution and incubated at 37 °C for 15 min. The fluorescence was measured with a spectrofluorophotometer at excitation and emission wavelengths of 485 and 525 nm. The fluorescence was normalized by OD_{600} and substituted into the following formula:

$$[1 - (\text{Fluorescence of treated sample}) / (\text{Fluorescence of untreated sample})] \times 100$$

2.9.1. Scanning electron microscopy (SEM) images analysis

SEM image analysis was conducted with a modified previous method (S.-H. Park and Kang, 2017). Treated (75 μM of quercetin only, 80 J/cm^2 of blue light only, and combined aPDT) or untreated pathogens in PBS were centrifuged at 10,000 \times g for 5 min to harvest cell pellet. Then, the samples were fixed in 2% Karnovsky's fixative for 24 h and washed three times with 0.05 M sodium cacodylate buffer for 10 min. For post-fixation, washed cells were immersed in a solution of 1% osmium tetroxide in 0.05 M cacodylate buffer for 2 h, and briefly washed thrice with distilled water. The fixed samples were dehydrated by immersing in a graded ethanol series (once in 30, 50, 70, 80, 90%, and thrice in 100%) for 5 min each, and then completely dried in a Hexamethyldisilazane. Dried samples were mounted on glass covered aluminum stubs and then sputter-coated with thin platinum layer (10 nm) using a vacuum coater (EM ACE200, Leica, Germany). SEM images were observed

using a Field-Emission Scanning Electron Microscope (SIGMA, Carl Zeiss, Germany).

2.10. Statistical analysis

All the experiments were performed thrice. The obtained data were analyzed using the Statistical Analysis System (version 9.4) (SAS Institute, Cary, NC, USA). The mean values were separated using the Duncan's multiple range test, and significant differences were determined at a probability level (P) of 0.05.

3. Results and discussion

3.1. Pathogen inactivation effects of quercetin mediated aPDT

The log reduction values of *E. coli* O157:H7 and *L. monocytogenes* at various concentrations of quercetin in PBS are depicted in Fig. 1. To determine an appropriate quercetin concentration, 50, 75, and 100 μM of quercetin combined with illumination were evaluated. At all concentrations, quercetin incubated in the dark for an amount of time corresponding to 80 J/cm^2 treatment resulted in the reduction of less than 1 log CFU/ml. However, a more than 4 log reduction for both bacteria occurred when three concentrations of quercetin combined with 80 J/cm^2 illuminations were treated. The highest reduction value was at a concentration of 75 μM at which a 6.20 and a >7.55 log reduction were observed for *E. coli* O157:H7 and *L. monocytogenes*, respectively. Therefore, all following experiments were investigated with 75 μM of quercetin.

The bactericidal effects of BL and BL combined with quercetin treatment were evaluated under different irradiation dosages. Fig. 2 shows the surviving populations of *E. coli* O157:H7 and *L. monocytogenes*. Compared to treatment with BL alone, the combination treatment significantly ($P < 0.05$) reduced the *E. coli* O157:H7 population under treatment doses from 40 to 80 J/cm^2 and the *L. monocytogenes* population under treatment doses from 20 to 80 J/cm^2 . The initial survival population of *E. coli* O157:H7 cells in the sample without quercetin was 7.20 log CFU/ml, which was diminished to 4.01 log CFU/ml after 80 J/cm^2 of illumination by BL (Fig. 2A). Illumination gradually reduced the number of cells in the sample treated with quercetin from 6.92 to 0.72 log CFU/ml. A similar trend was observed for *L. monocytogenes* (Fig. 2B) under BL illumination without quercetin

treatment, where a 2.91 log reduction was obtained at 80 J/cm^2 . However, the population of *L. monocytogenes* cells in the sample containing quercetin was drastically decreased under 40 J/cm^2 illumination. No cells were detected at 80 J/cm^2 illumination (the limit of detection is 1 CFU/ml).

Microbial reduction after quercetin mediated aPDT in liquid food samples were indicated in Figs. 3 and 4. In milk disinfection, the number of *E. coli* O157:H7 was reduced by 2.40 log CFU/ml and that of *L. monocytogenes* was reduced by 0.50 log CFU/ml after individual BL treatment at 80 and 120 J/cm^2 respectively, while the number of *E. coli* O157:H7 was reduced by 5.01 log CFU/ml and that of *L. monocytogenes* was reduced by 1.93 log CFU/ml after aPDT at 80 and 120 J/cm^2 respectively. In white grape juice disinfection, the number of *E. coli* O157:H7 was reduced by 2.98 log CFU/ml and that of *L. monocytogenes* was reduced by 0.66 log CFU/ml after individual BL treatment at 40 J/cm^2 respectively, while the number of *E. coli* O157:H7 was reduced by 5.46 log CFU/ml and that of *L. monocytogenes* was reduced by 5.98 log CFU/ml after aPDT at 40 J/cm^2 respectively.

Notably, after 2h of recovery in TSB, *E. coli* O157:H7 in milk and white grape juice was significantly ($P < 0.05$) resuscitated by 1.29 and 1.36 log CFU/ml. This data was in the same vein as the previous study that reported occurrence of *E. coli* O157:H7 injured cells after quercetin mediated aPDT in apple juice. Since antioxidant enzyme such as superoxide dismutase and catalase can detoxify ROS and relieve oxidative stress, ROS mediated treatment induced injured cells in *E. coli* O157:H7 (Shi et al., 2019; Z. Zhang et al., 2022). The question still remains why the aPDT efficacy to control *L. monocytogenes* was only achieved around 2 log reduction. Milk contain various nutrients such as protein, lipid, and polysaccharide, and among these nutrients, some peptides have ability to quench ROS (Yujia et al., 2022). It is inferred that *L. monocytogenes* showed higher resistance in milk because ROS quenching effect were more pronounced against gram positive bacteria (Huang et al., 2012).

The microbicidal effect of quercetin mediated aPDT combined with EDTA is shown in Fig. 5. The survival population values of the sample treated by aPDT with EDTA are significantly ($P < 0.05$) lower than those without EDTA for *E. coli* O157:H7 from 40 J/cm^2 . Conversely, there is no significant ($P > 0.05$) difference at every dose for the survival population values of *L. monocytogenes* treated by aPDT with or without EDTA.

The antimicrobial effect of the quercetin and BL combination treatment was evaluated at various quercetin concentrations and under different illumination dosages. The schematic diagram of treatment and

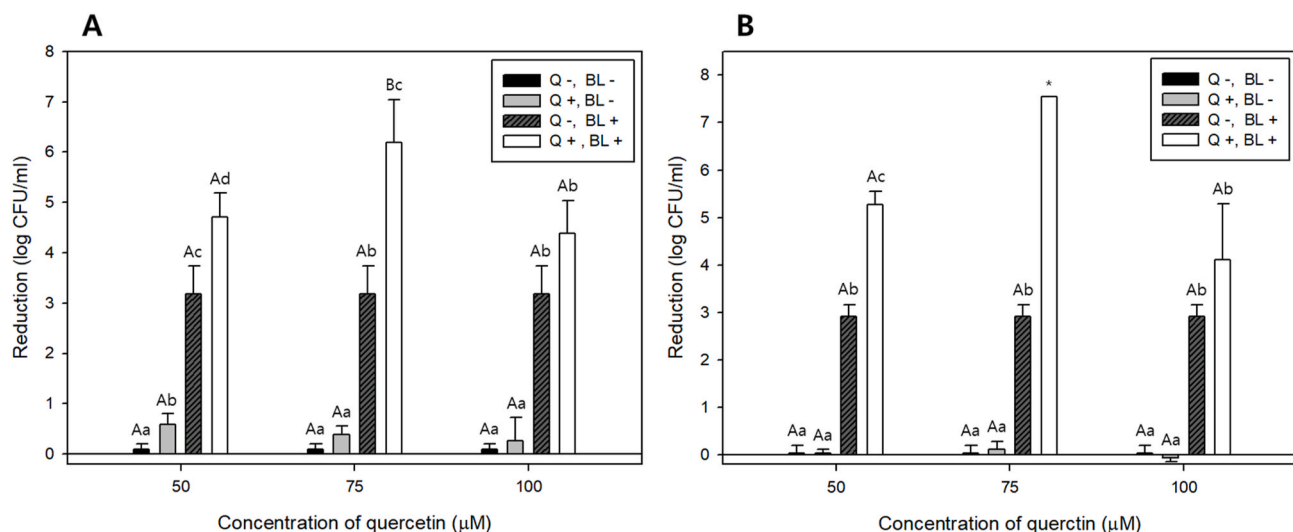


Fig. 1. The microbial reduction of (A) *E. coli* O157:H7 and (B) *L. monocytogenes* after aPDT at 80 J/cm^2 with three different concentrations of quercetin (50, 75, and 100 μM). Asterisk represented that the cells were not detectable. The error bars represent the standard deviation, and the data correspond to the averaged results of three independent experiments. Different uppercase letters indicate significant ($P < 0.05$) differences for the same treatment. Different lowercase letters indicate significant ($P < 0.05$) differences for different treatments with the same light dose. Q: quercetin and BL: blue light.

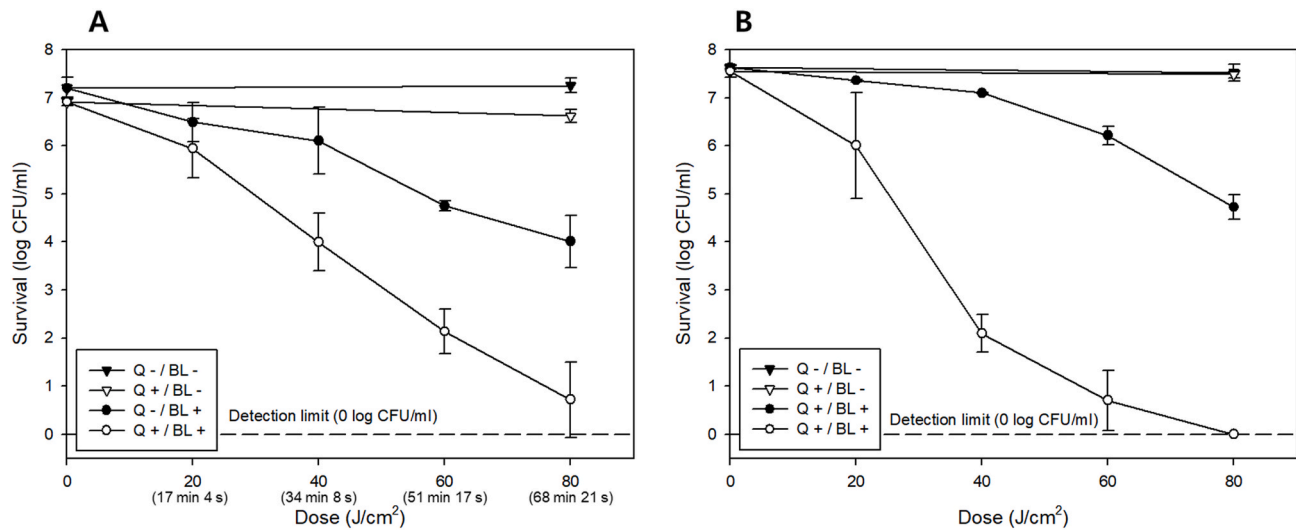


Fig. 2. Survival population of (A) *E. coli* O157:H7 and (B) *L. monocytogenes* after aPDT with and without 75 μ M quercetin. The error bars represent the standard deviation, and the data correspond to the averaged results of three independent experiments. Q: quercetin and BL: blue light.

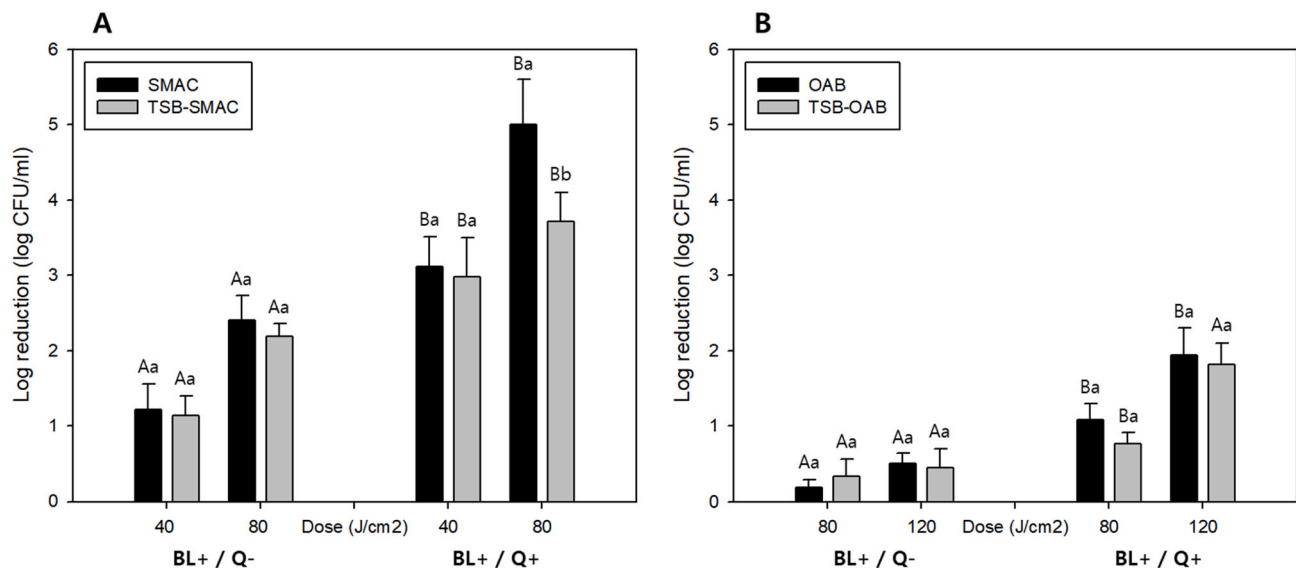


Fig. 3. The microbial reduction of (A) *E. coli* O157:H7 and (B) *L. monocytogenes* in milk after aPDT with and without 75 μ M quercetin or blue light. The error bars represent the standard deviation, and the data correspond to the averaged results of three independent experiments. Different uppercase letters indicate significant ($P < 0.05$) differences between blue light treatment with or without quercetin. Different lowercase letters indicate significant ($P < 0.05$) differences between treatments with recovery or not. Q: quercetin and BL: blue light.

the absorbance of quercetin and emission spectra of 405 nm LEDs were presented in Fig. S1. While no reduction was observed until using 100 μ M quercetin without illumination, 75 μ M quercetin was significantly ($P < 0.05$) more effective to decrease bacteria cells than the other two concentrations when irradiated (Fig. 1). Therefore, 75 μ M quercetin was selected as mentioned above. The reason that 100 μ M quercetin was less effective than 75 μ M quercetin is supposed to be due to its low solubility. Quercetin is barely soluble in water and its aggregation is observed at high concentrations. Therefore, This aggregation interrupted the light from reaching bacteria and quercetin molecules and decreased inactivation efficacy (Temba et al., 2016).

BL has previously been used to disinfect pathogens. Quercetin was used as an exogenous PS in the present study to enhance the antimicrobial effect of BL irradiation. The combination treatment resulted in an additional maximum reduction of 3.01 log for *E. coli* O157:H7 at a dose of 80 J/cm² and of 5.52 log for *L. monocytogenes* at a dose of 60 J/cm² compared to BL treatment (Fig. 2). The BL treatment alone may inactivate the cells by their own endogenous porphyrins (Maclean et al., 2014). In this result, there is no different microbial reduction between the both bacteria after 80 J/cm² BL treatment alone ($P > 0.05$). However, after aPDT with same irradiance dose, *L. monocytogenes* were reduced below detection limit, whereas *E. coli* O157:H7 were not. More time was required to obtain a more than 5 log reduction of the bacterial cells for *E. coli* O157:H7 than for *L. monocytogenes*. That is, *E. coli* O157:H7 was more resistant than *L. monocytogenes* to aPDT with quercetin. The result was inferred to be from the difference in the cell wall structures between the bacteria. This is because the external bacterial structure is a primary target of the ROS produced by a hydrophobic exogenous PS which is difficult to diffuse into cells, such as curcumin (Ghate et al., 2019; Maraccini et al., 2016). Gram-negative bacteria have an outer membrane that consists of LPS, phospholipids, and lipoproteins outside a thin peptidoglycan layer. EDTA induce the loss of

cm² compared to BL treatment (Fig. 2). The BL treatment alone may inactivate the cells by their own endogenous porphyrins (Maclean et al., 2014). In this result, there is no different microbial reduction between the both bacteria after 80 J/cm² BL treatment alone ($P > 0.05$). However, after aPDT with same irradiance dose, *L. monocytogenes* were reduced below detection limit, whereas *E. coli* O157:H7 were not. More time was required to obtain a more than 5 log reduction of the bacterial cells for *E. coli* O157:H7 than for *L. monocytogenes*. That is, *E. coli* O157:H7 was more resistant than *L. monocytogenes* to aPDT with quercetin. The result was inferred to be from the difference in the cell wall structures between the bacteria. This is because the external bacterial structure is a primary target of the ROS produced by a hydrophobic exogenous PS which is difficult to diffuse into cells, such as curcumin (Ghate et al., 2019; Maraccini et al., 2016). Gram-negative bacteria have an outer membrane that consists of LPS, phospholipids, and lipoproteins outside a thin peptidoglycan layer. EDTA induce the loss of

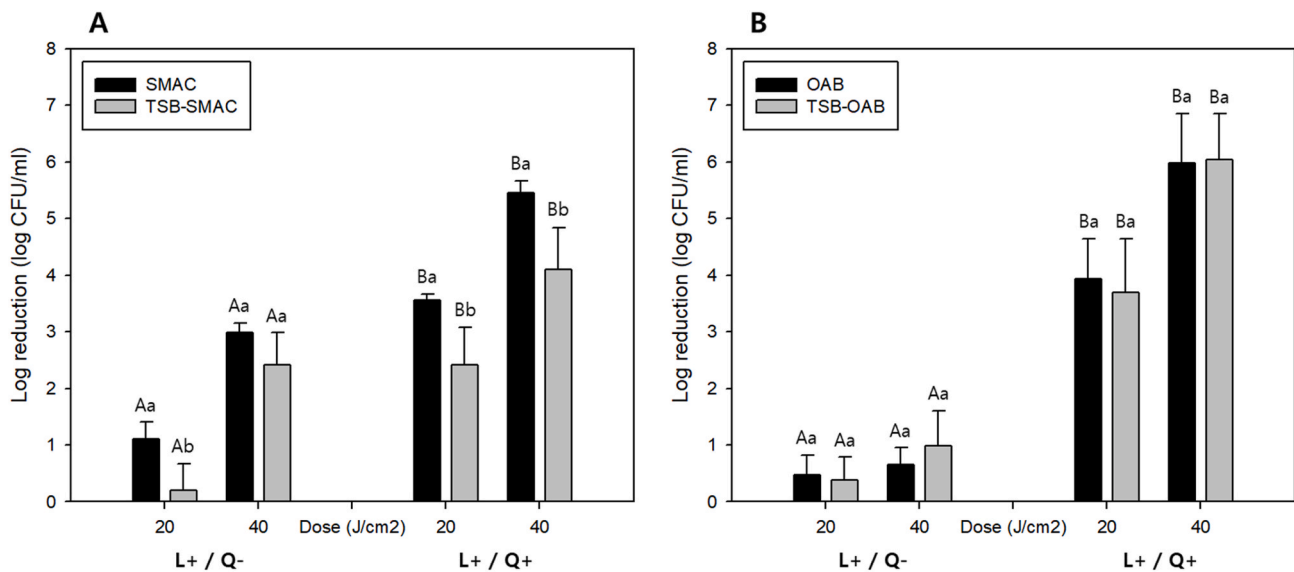


Fig. 4. The microbial reduction of (A) *E. coli* O157:H7 and (B) *L. monocytogenes* in white grape juice after aPDT with and without 75 μ M quercetin or blue light. The error bars represent the standard deviation, and the data correspond to the averaged results of three independent experiments. Different uppercase letters indicate significant ($P < 0.05$) differences between blue light treatment with or without quercetin. Different lowercase letters indicate significant ($P < 0.05$) differences between treatments with recovery or not. Q: quercetin and BL: blue light.

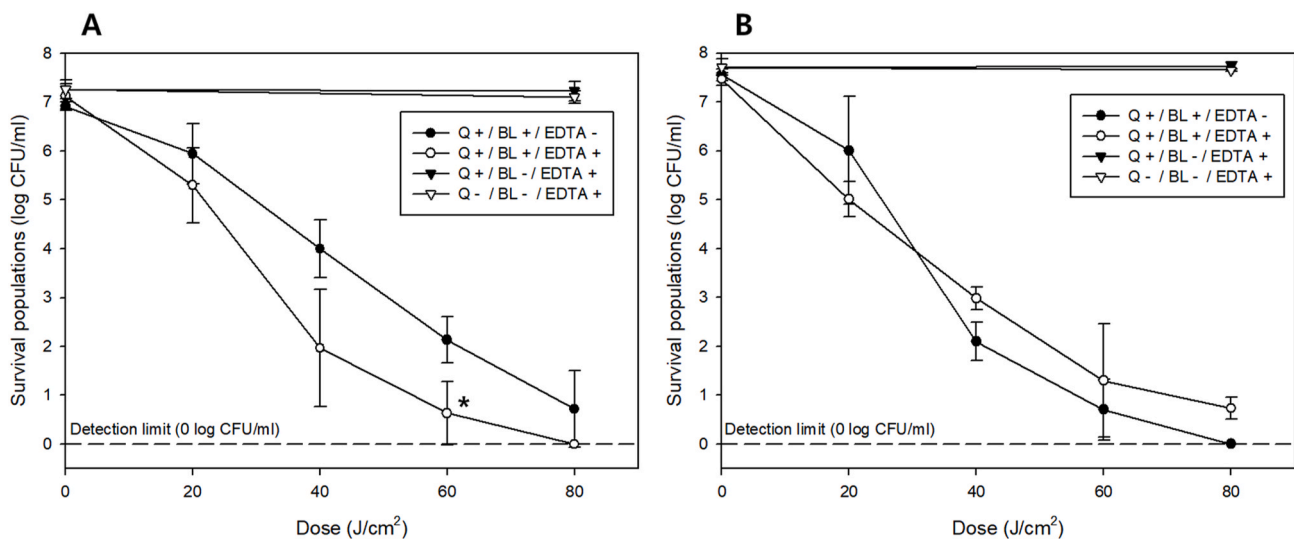


Fig. 5. Survival population of (A) *E. coli* O157:H7 and (B) *L. monocytogenes* after aPDT with 75 μ M quercetin and with or without EDTA 1 mM. Asterisk represented that there was significant ($P < 0.05$) difference between the samples with and without EDTA 1 mM treated BL. The error bars represent the standard deviation, and the data correspond to the averaged results of three independent experiments. Q: quercetin and BL: blue light.

interaction between LPS molecules by replacing divalent cation (Khan et al., 2015). In Fig. 3, *E. coli* O157:H7 cells which had malfunctioned LPS significantly ($P < 0.05$) more reduced by aPDT at 60 J/cm^2 . From this result, it is demonstrated that LPS on the outer membrane of Gram-negative bacteria operate as a physically protective barrier against oxidative damage by ROS produced by aPDT. Moreover, the LPS of Gram-negative bacteria and the peptidoglycan layer of Gram-positive bacteria make different accessibility of photosensitizer (Penha et al., 2017). The anionically charged LPS inhibits the hydrophobic quercetin molecule from accessing bacteria, making ROS, with a short half-life, ineffective against bacteria, by contrast, the porous peptidoglycan cell wall is more readily for quercetin to bind and penetration through the cells (Gao and Matthews, 2020). Therefore, the degradation of LPS is necessary for enhancing inactivation efficacy. A previous study showed that the antimicrobial activity of gallic acid and UV-A (365 nm) was

enhanced by removing the outer membrane and the permeability was increased using EDTA (Q. Wang et al., 2017). In another study, positively charged riboflavin derivatives were used to enhance the antimicrobial activity of aPDT (Maisch et al., 2014). There were negligible differences between the quantum yield of riboflavin derivatives with one and eight positive charges (0.75 ± 0.05 and 0.78 ± 0.05 , respectively), although using a positively charged PS resulted in higher bacterial reduction. It was suggested that the positively charged PS facilitated the approach of PS to the anionic LPS, thereby enhancing the antimicrobial effect. In summary, although *E. coli* O157:H7 was more resistant to quercetin mediated aPDT than *L. monocytogenes*, it was shown that quercetin and BL effectively reduced both bacteria.

3.2. Evaluation of ROS production

The means by which energy is transferred to a PS during irradiation determines the dominant ROS for inactivation. Because ROS can react with bacteria cells, for accurate measurement, the ROS production was estimated without bacteria cells (Fig. 6). The production $^1\text{O}_2$ results in the oxidation of imidazole, followed by oxidation of RNO which has a maximum absorbance at 440 nm, thereby decreasing the absorbance at 440 nm (Kraljić and Mohsni, 1978). The reduction in absorbance of the sample treated with quercetin alone, or with quercetin and BL irradiation higher than that of the untreated sample except at 20 J/cm². There was no significant difference ($P > 0.05$) between the absorbance of the sample treated with quercetin with and without irradiation except at 40 J/cm² (Fig. 6A). The generation of $\text{O}_2^{\bullet-}$ was evaluated using XTT (Fig. 6B). The reduction of water insoluble XTT tetrazolium to water-soluble XTT formazan by $\text{O}_2^{\bullet-}$ increases the absorbance at 470 nm (Sutherland and Learmonth, 1997; Ukeda et al., 1997). There was a significant ($P < 0.05$) increase in the absorbance of the samples under all conditions except for the control. The quercetin and BL combination treatment produced the significantly ($P < 0.05$) highest absorbance at every dose, followed by the sample treated with quercetin alone. Ellman's reagent, DTNB, was used to measure the generation of H_2O_2 (Riddles et al., 1979). DTNB can react with the thiol group (-SH) of GSH and is converted to 2-nitro-5-thiobenzoic acid (TNB), which can be quantified by the absorbance at 412 nm. The oxidation of GSH to a disulfide bond (GS-SG) prevents TNB production, thereby decreasing the absorbance at 412 nm. The GSH loss significantly ($P < 0.05$) increased using the quercetin and illumination combination treatment (Fig. 6C). The maximum loss of GSH (45.1%) was observed at 80 J/cm².

In a previous study, 9,10-anthracenediyl-bis (methylene) dimalonic acid (ADMA) was used to detect of generation of $^1\text{O}_2$ when a 10 μM curcumin solution was activated by 470-nm BL (Wu et al., 2016). The spectra obtained in our study using reagents without cells were used to classify quercetin as a type I dominant PS in solution. In RNO bleaching method, the absorbance of both the treated sample with the BL and quercetin combination treatment and the sample incubated in the dark with quercetin was decreased. Lagunes et al. (Lagunes and Trigos, 2015) used an indirect method of ergosterol oxidation to determine the $^1\text{O}_2$ -production of quercetin in the presence of the visible light (380–780 nm). In the present study, the generation of $^1\text{O}_2$ was not significantly ($P > 0.05$) different with and without irradiation. The increase in the absorbance of XTT formazan at 470 nm occurred under the quercetin and BL combination treatment as well as for incubation in the dark with quercetin. However, a reduction in the bacterial population was not observed after incubation in the dark. It was demonstrated in a previous study that the 3-(4,5-dimethylthiazol-2-yl)-2,5-diphenyl

tetrazolium bromide (MTT) tetrazolium salt, which had been used for estimating living cells, was reduced by quercetin in the absence of living cells (Peng et al., 2005). MTT and XTT have similar structures and have both been used to measure cell viability and superoxide formation (S. Wang et al., 2011). Therefore, quercetin may reduce XTT tetrazolium to formazan in the absence of illumination, thereby increasing the absorbance at 470 nm. The quercetin and BL combination treatment resulted in a significantly ($P < 0.05$) higher reduction of XTT tetrazolium than by incubation with quercetin in the dark. This result showed that XTT tetrazolium reduction is caused by produced $\text{O}_2^{\bullet-}$ as well as quercetin. The production of $\text{O}_2^{\bullet-}$ and H_2O_2 significantly ($P < 0.05$) increased with the dose. Thus, the ROS produced by the quercetin and illumination combination treatment were $\text{O}_2^{\bullet-}$ and H_2O_2 , where quercetin in solution is a type I dominant PS.

3.3. Estimation of quercetin uptake in bacterial cells

DPBA fluorescence was used to estimate the quercetin uptake in *E. coli* O157:H7 and *L. monocytogenes* as the irradiation dose was increased (Fig. 7). The results for *E. coli* O157:H7 cells (Fig. 7A) without irradiation were not significantly ($P > 0.05$) different from those for untreated cells. By contrast, the results were significantly ($P < 0.05$) different for *L. monocytogenes* (Fig. 7B) between untreated cells and incubated cells in the dark at the time same as 60 J/cm² and 80 J/cm². Irradiation with BL at 40 J/cm² and 20 J/cm² for *E. coli* O157:H7 and *L. monocytogenes*, respectively, significantly ($P < 0.05$) started to increase the fluorescence.

The interaction of bacteria cells and quercetin was estimated using DPBA. The results show that external quercetin did not diffuse into the inner space of the Gram-negative bacteria in the absence of illumination. This result provides evidence that negatively charged LPS prevents the hydrophobic molecule from accessing Gram-negative bacteria (F Sperandio, Huang, & R Hamblin, 2013). Compared to this result, quercetin diffused into the Gram-positive cells over time. However, under BL irradiation, quercetin diffused into the cells significantly ($P < 0.05$) faster. When BL was irradiated, the significant ($P < 0.05$) increase in quercetin uptake occurred in *L. monocytogenes* cells after 20 J/cm² treatment and in *E. coli* O157:H7 cells after 40 J/cm² treatment. The increased quercetin uptake may be due to the damage to the cell wall and outer membrane by the produced ROS as described in section 3.4. In summary, quercetin was localized out of the cell before illumination. Externally produced ROS damaged the cell membrane, making the cell membrane permeable, and then quercetin diffused into the cell.

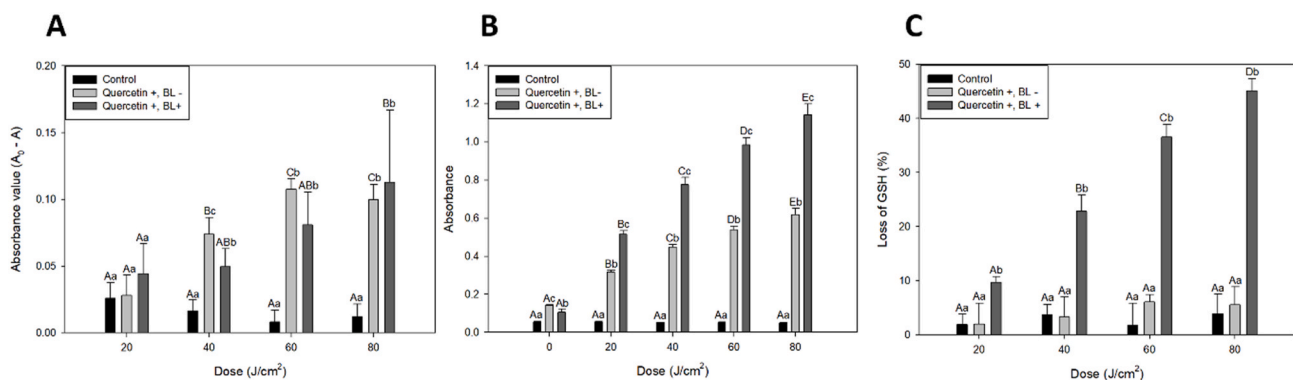


Fig. 6. Evaluation of ROS production. (A) The reduction in the absorbance at a wavelength of 440 nm ($A_0 - A$) due to the decrease in RNO by $^1\text{O}_2$. (B) The absorbance of XTT at a wavelength of 470 nm was reduced by the action of $\text{O}_2^{\bullet-}$. (C) The oxidation of GSH by H_2O_2 using Ellman's reagent ($(A_0 - A)/A_0 \times 100$). The error bars represent the standard deviation, and the data correspond to the averaged results of three independent experiments. Different uppercase letters indicate significant ($P < 0.05$) differences for the same treatment. Different lowercase letters indicate significant ($P < 0.05$) differences for different treatments with the same light dose. Q: quercetin and BL: blue light. Unit of absorbance: AU.

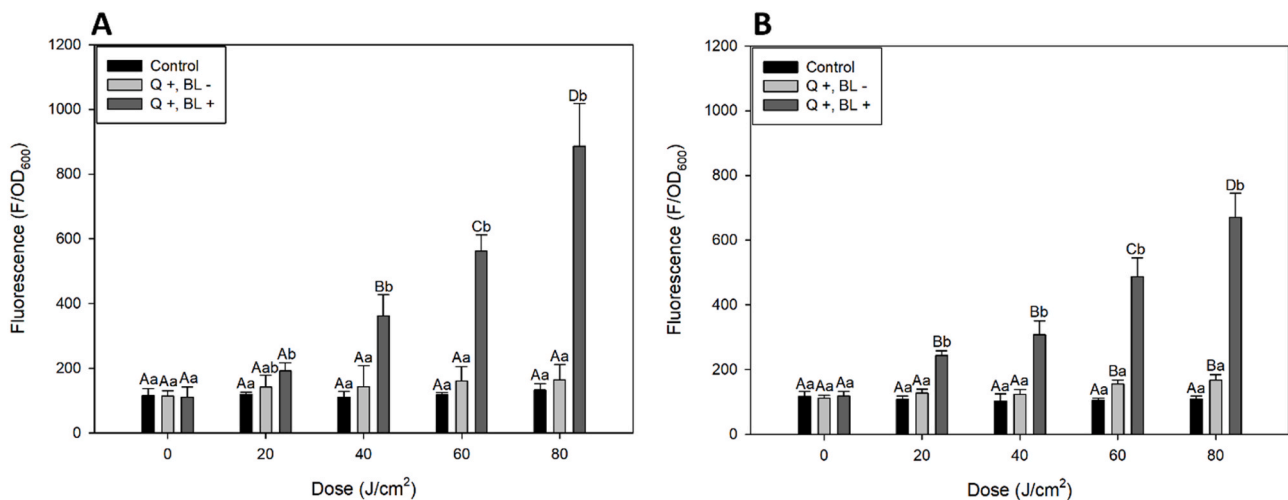


Fig. 7. The uptake of quercetin bound to DBPA in (A) *E. coli* O157:H7 and (B) *L. monocytogenes* at an excitation wavelength of 480 nm and an emission wavelength of 535 nm. The measured fluorescence was normalized by OD₆₀₀. The error bars represent the standard deviation, and the data correspond to the averaged results of three independent experiments. Different uppercase letters indicate significant ($P < 0.05$) differences for the same treatment. Different lowercase letters indicate significant ($P < 0.05$) differences for different treatments with the same light dose. Q: quercetin and BL: blue light.

3.4. Assessment of cell membrane and DNA damage

Fig. 8 shows the damage to the bacterial cell membrane resulting from the quercetin and BL combination treatment assessed using PI. There was no significant ($P > 0.05$) increase in the fluorescence for both bacteria by treatment with quercetin alone and BL illumination alone. A significant ($P < 0.05$) increase in the fluorescence was obtained for both *E. coli* O157:H7 cells and *L. monocytogenes* cells under quercetin combined with BL treatment at 40 J/cm². SEM image analysis was performed to provide visual information on cell membrane damage. As shown in Fig. 9, while untreated cells revealed smooth cell surfaces without flaw (Fig. 9A and D), disruption or distorted spots were observed in cell outer membrane of *E. coli* O157:H7 (Fig. 9B and C) or cell wall of *L. monocytogenes* (Fig. 9E and F). Zhang et al. (2022) also observed distorted surface and pore in *E. coli* O157:H7 membrane after photodynamic treatment (Z. Zhang et al., 2022)

The loss of the DNA integrity of bacteria by aPDT is depicted in Fig. 10. There is no decrease in the DNA integrity of both bacteria after

incubation with quercetin in dark for 68 min 21 s. On the contrary, BL and quercetin mediated aPDT at 80 J/cm² damaged the bacterial DNA. For *E. coli* O157:H7, the loss of DNA integrity was significantly ($P < 0.05$) higher after quercetin mediated aPDT (84.38%) than BL treatment (38.78%). The DNA integrity of *L. monocytogenes* was consistent with the result of *E. coli* O157:H7. The loss rate after quercetin mediated aPDT (84.08%) was significantly higher than that of after BL treatment (33.45%).

In this study, significant membrane damage was not observed ($P > 0.05$) under BL treatment without quercetin or incubation with quercetin in the dark. By contrast, the increase in the PI fluorescence under aPDT using quercetin verified that this treatment damages the bacterial cell membrane. This result is consistent with interpretation of the result of quercetin uptake and indicates that quercetin uptake by cells increased with the membrane permeability increased due to membrane damage. In the meantime, different inactivation mechanisms were confirmed for endogenous and exogenous PSs. BL treatment reduced the *E. coli* O157:H7 and *L. monocytogenes* cell populations by approximately

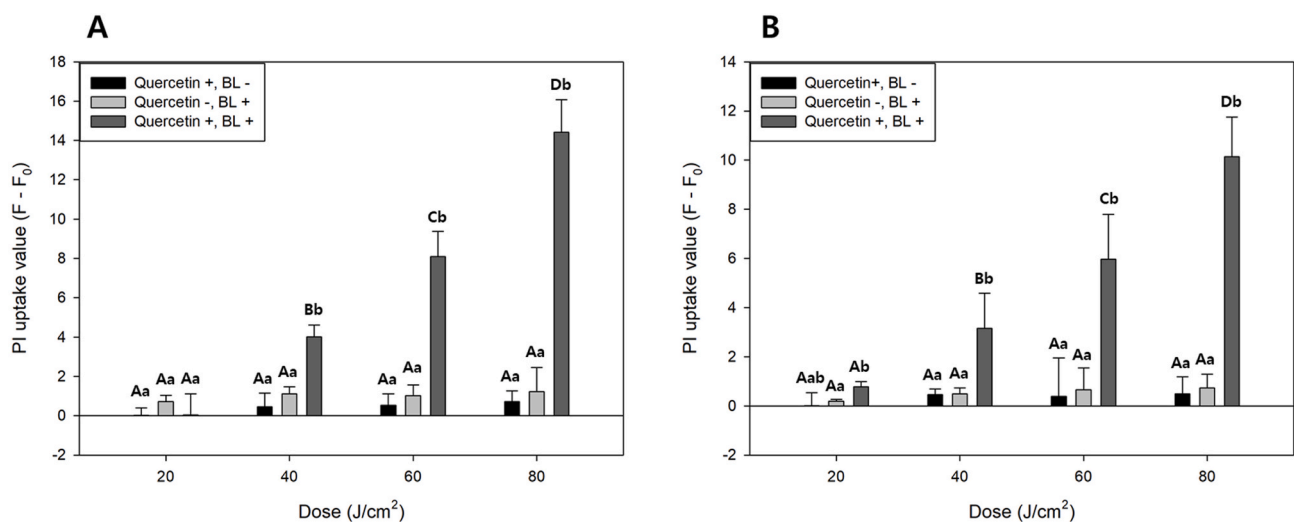


Fig. 8. Measurement of membrane integrity of (A) *E. coli* O157:H7 and (B) *L. monocytogenes* under different treatments and doses using a PI assay. The fluorescence was normalized by OD₆₀₀ and substituted into the following formula: (fluorescence of treated sample/OD₆₀₀ (F)) – (fluorescence of untreated sample/OD₆₀₀ (F₀)). Different uppercase letters indicate significant ($P < 0.05$) differences for the same treatment. Different lowercase letters indicate significant ($P < 0.05$) differences for different treatments with the same light dose. Q: quercetin and BL: blue light.

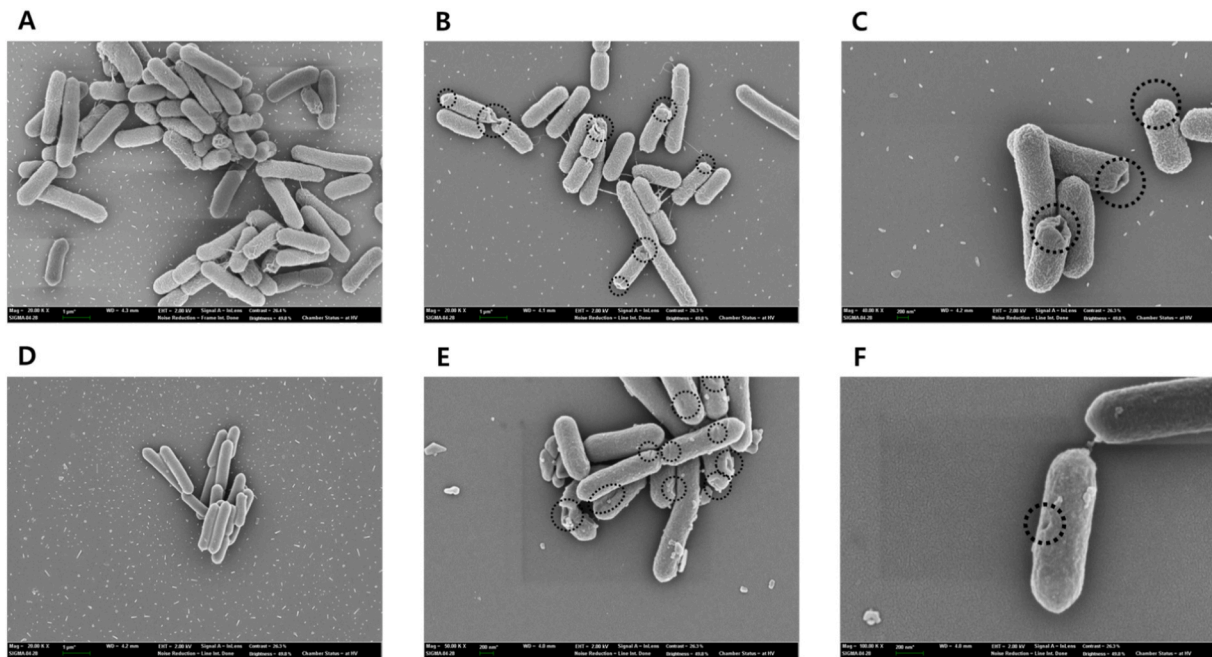


Fig. 9. SEM images analysis of (A, B, C) *E. coli* O157:H7 and (D, E, F) *L. monocytogenes* (A, D) before and (B, C, E, F) after quercetin mediated aPDT. Black dotted circles indicate damaged spot in cell membrane. Magnifications were 20,000 \times (A, B, D), 40,000 \times (C, E) and 100,000 \times (F).

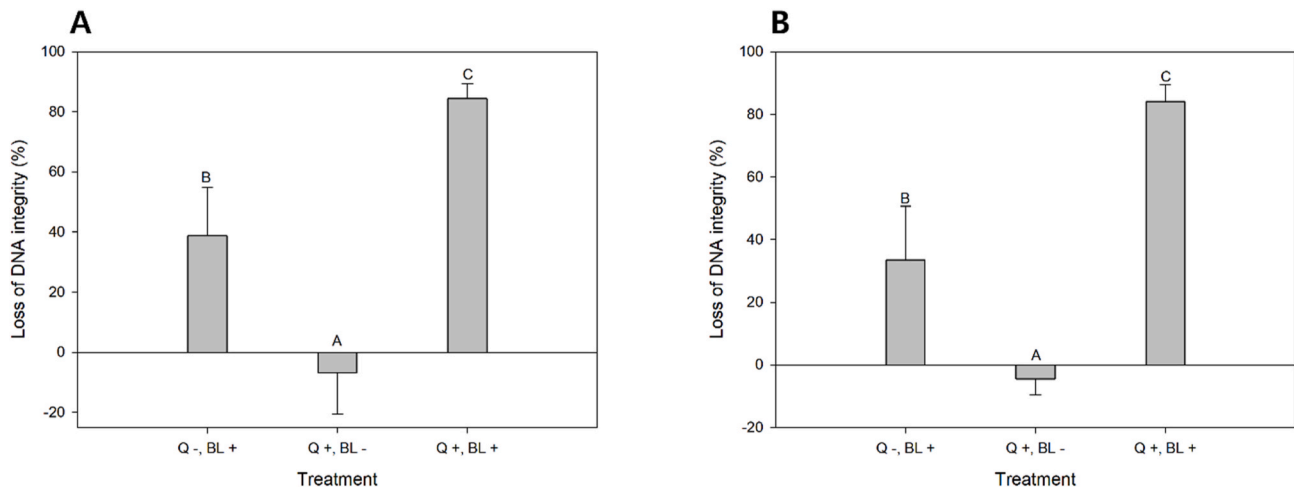


Fig. 10. DNA integrity of (A) *E. coli* O157:H7 and (B) *L. monocytogenes* after aPDT in PBS. An excitation wavelength was 485 nm and an emission wavelength was 525 nm. The measured fluorescence was normalized by OD₆₀₀. The error bars represent the standard deviation, and the data correspond to the averaged results of three independent experiments. Different uppercase letters indicate significant ($P < 0.05$) differences for the different treatment. Q: quercetin and BL: blue light.

3 log CFU/ml, however, there was no significant ($P > 0.05$) increase in PI uptake. On the contrary to the result of the membrane damage assay, there was a significant ($P < 0.05$) decrease in DNA integrity after BL treatment in this study. Endogenous PSs generate intracellular ROS that inactivates bacteria by oxidizing materials in bacterial cells, such as nucleic acids and proteins, rather than the outer membrane (Ferrer-Espada et al., 2019). Nevertheless, quercetin mediated aPDT damaged significantly ($P < 0.05$) bacterial DNA more than BL treatment alone. In conclusion, quercetin, an Exogenous PS, was located outside bacterial cells, therefore, produce ROS that started to attack the bacterial cell from the outermost structure. After that, the diffusion of quercetin into damaged bacteria occurred and ROS produced by the entered quercetin damaged bacterial DNA.

4. Conclusion

The antimicrobial effect of quercetin mediated aPDT using a 405 nm BL LED was evaluated in this study. Over a 5 log reduction was achieved for both *E. coli* O157:H7 and *L. monocytogenes* in a buffer solution. The bacterial inactivation depended on the illumination dose. The inactivation mechanism was the membrane damage by produced ROS, which were $O_2^{\bullet-}$ and H_2O_2 for a type I dominant mechanism. The measured quercetin uptake showed that ROS were produced outside cells, which was consistent with the membrane damage assessment. These results indicated that the ROS damaged the outer cell structures. Based on these results, further studies, such as applications to food surfaces or liquid foods, are needed to apply to food as a nonthermal technology to prevent microbial contamination in the food safety field.

CRedit authorship contribution statement

In-Hwan Lee: Conceptualization, Methodology, Data curation, Investigation, Writing – original draft. **Soo-Hwan Kim:** Validation, Data curation, Writing – review & editing. **Dong-Hyun Kang:** Supervision, Funding acquisition, Methodology.

Declaration of competing interest

The authors declare that they have no known competing financial interests or personal relationships that could have appeared to influence the work reported in this paper.

Data availability

No data was used for the research described in the article.

Acknowledgements

This work was carried out with the support of Cooperative Research Program for Agriculture Science & Technology Development (Project No. PJ01608203) of Rural Development Administration, Republic of Korea.

Appendix A. Supplementary data

Supplementary data to this article can be found online at <https://doi.org/10.1016/j.crfs.2022.100428>.

References

- Amin, R.M., Bhayana, B., Hamblin, M.R., Dai, T., 2016. Antimicrobial blue light inactivation of *Pseudomonas aeruginosa* by photo-excitation of endogenous porphyrins: in vitro and in vivo studies. *Laser Surg. Med.* 48 (5), 562–568.
- Boots, A.W., Haenen, G.R., Bast, A., 2008. Health effects of quercetin: from antioxidant to nutraceutical. *Eur. J. Pharmacol.* 585 (2–3), 325–337.
- Brovko, L., 2010. Photodynamic treatment: a new efficient alternative for surface sanitation. *Adv. Food Nutr. Res.* 61, 119–147.
- Buer, C.S., Imin, N., Djordjevic, M.A., 2010. Flavonoids: new roles for old molecules. *J. Integr. Plant Biol.* 52 (1), 98–111.
- Cho, E.-R., Kang, D.-H., 2022. Intensified inactivation efficacy of pulsed ohmic heating for pathogens in soybean milk due to sodium lactate. *Food Control* 137, 108936.
- Condat, M., Babinot, J., Tomane, S., Malval, J.-P., Kang, I.-K., Spillebout, F., Mazeran, P.-E., Lalevée, J., Andalloussi, S.A., Versace, D.-L., 2016. Development of photoactivable glycerol-based coatings containing quercetin for antibacterial applications. *RSC Adv.* 6 (22), 18235–18245.
- de Oliveira, E.F., Tosati, J.V., Tikekar, R.V., Monteiro, A.R., Nitin, N., 2018. Antimicrobial activity of curcumin in combination with light against *Escherichia coli* O157: H7 and *Listeria innocua*: applications for fresh produce sanitation. *Postharvest Biol. Technol.* 137, 86–94.
- Delorme, M.M., Guimarães, J.T., Coutinho, N.M., Balthazar, C.F., Rocha, R.S., Silva, R., Margalho, L.P., Pimentel, T.C., Silva, M.C., Freitas, M.Q., 2020. Ultraviolet radiation: an interesting technology to preserve quality and safety of milk and dairy foods. *Trends Food Sci. Technol.* 102, 146–154.
- Deprez, R.H.L., Fijnvandraat, A.C., Ruijter, J.M., Moorman, A.F., 2002. Sensitivity and accuracy of quantitative real-time polymerase chain reaction using SYBR green I depends on cDNA synthesis conditions. *Anal. Biochem.* 307 (1), 63–69.
- Dias, L.D., Blanco, K.C., Mfouo-Tynga, I.S., Inada, N.M., Bagnato, V.S., 2020. Curcumin as a photosensitizer: from molecular structure to recent advances in antimicrobial photodynamic therapy. *J. Photochem. Photobiol. C Photochem. Rev.*, 100384.
- F Sperandio, F., Huang, Y.-Y., R Hamblin, M., 2013. Antimicrobial photodynamic therapy to kill Gram-negative bacteria. *Recent Pat. Anti-Infect. Drug Discov.* 8 (2), 108–120.
- Ferrer-Espada, R., Liu, X., Goh, X.S., Dai, T., 2019. Antimicrobial blue light inactivation of polymicrobial biofilms. *Front. Microbiol.* 10, 721.
- Gao, J., Matthews, K.R., 2020. Effects of the photosensitizer curcumin in inactivating foodborne pathogens on chicken skin. *Food Control* 109, 106959.
- Ghate, V.S., Zhou, W., Yuk, H.G., 2019. Perspectives and trends in the application of photodynamic inactivation for microbiological food safety. *Compr. Rev. Food Sci. Food Saf.* 18 (2), 402–424.
- Hamblin, M.R., 2016. Antimicrobial photodynamic inactivation: a bright new technique to kill resistant microbes. *Curr. Opin. Microbiol.* 33, 67–73.
- Han, J.Y., Song, W.J., Kang, D.H., 2019. Optimization of broth recovery for repair of heat-injured *Salmonella enterica* serovar Typhimurium and *Escherichia coli* O157: H7. *J. Appl. Microbiol.* 126 (6), 1923–1930.
- Hu, J., Lin, S., Tan, B.K., Hamzah, S.S., Lin, Y., Kong, Z., Zhang, Y., Zheng, B., Zeng, S., 2018. Photodynamic inactivation of *Burkholderia cepacia* by curcumin in combination with EDTA. *Food Res. Int.* 111, 265–271.
- Huang, L., Xuan, Y., Koide, Y., Zhiyentayev, T., Tanaka, M., Hamblin, M.R., 2012. Type I and Type II mechanisms of antimicrobial photodynamic therapy: an in vitro study on gram-negative and gram-positive bacteria. *Laser Surg. Med.* 44 (6), 490–499.
- Khan, A., Vu, K.D., Riedl, B., Lacroix, M., 2015. Optimization of the antimicrobial activity of nisin, Na-EDTA and pH against gram-negative and gram-positive bacteria. *LWT—Food Sci. Technol.* 61 (1), 124–129.
- Kim, S.-S., Shin, M., Kang, J.-W., Kim, D.-K., Kang, D.-H., 2020. Application of the 222 nm krypton-chlorine excilamp and 280 nm UVC light-emitting diode for the inactivation of *Listeria monocytogenes* and *Salmonella* Typhimurium in water with various turbidities. *Lebensm. Wiss. Technol.* 117, 108458.
- Kolodziejek, A.M., Minnich, S.A., Hovde, C.J., 2022. *Escherichia coli* O157: H7 virulence factors and the ruminant reservoir. *Curr. Opin. Infect. Dis.* 35 (3), 205–214.
- Kraljić, I., Mohsni, S.E., 1978. A new method for the detection of singlet oxygen in aqueous solutions. *Photochem. Photobiol.* 28 (4-5), 577–581.
- Lagunes, I., Trigos, Á., 2015. Photo-oxidation of ergosterol: indirect detection of antioxidants photosensitizers or quenchers of singlet oxygen. *J. Photochem. Photobiol. B Biol.* 145, 30–34.
- Lesjak, M., Beara, I., Simin, N., Pintać, D., Majkić, T., Bekvalac, K., Orčić, D., Mimica-Dukić, N., 2018. Antioxidant and anti-inflammatory activities of quercetin and its derivatives. *J. Funct. Foods* 40, 68–75.
- Liu, Y., Xiong, L., Kontopodi, E., Boeren, S., Zhang, L., Zhou, P., Hettinga, K., 2020. Changes in the milk serum proteome after thermal and non-thermal treatment. *Innovat. Food Sci. Emerg. Technol.* 66, 102544.
- Lui, G.Y., Roser, D., Corkish, R., Ashbolt, N.J., Stuetz, R., 2016. Point-of-use water disinfection using ultraviolet and visible light-emitting diodes. *Sci. Total Environ.* 553, 626–635.
- Luksienė, Z., Zukauskas, A., 2009. Prospects of photosensitization in control of pathogenic and harmful micro-organisms. *J. Appl. Microbiol.* 107 (5), 1415–1424.
- Maclean, M., McKenzie, K., Anderson, J.G., Gettinby, G., MacGregor, S.J., 2014. 405 nm light technology for the inactivation of pathogens and its potential role for environmental disinfection and infection control. *J. Hosp. Infect.* 88 (1), 1–11.
- Maisch, T., Eichner, A., Späth, A., Gollmer, A., König, B., Regensburger, J., Bäumlner, W., 2014. Fast and effective photodynamic inactivation of multiresistant bacteria by cationic riboflavin derivatives. *PLoS One* 9 (12), e111792.
- Maraccini, P.A., Wenk, J., Boehm, A.B., 2016. Photoinactivation of eight health-relevant bacterial species: determining the importance of the exogenous indirect mechanism. *Environ. Sci. Technol.* 50 (10), 5050–5059.
- Mostafidi, M., Sanjabi, M.R., Shir Khan, F., Zahedi, M.T., 2020. A review of recent trends in the development of the microbial safety of fruits and vegetables. *Trends Food Sci. Technol.* 103, 321–332.
- Nima, G., Soto-Montero, J., Alves, L.A., Mattos-Graner, R.O., Giannini, M., 2021. Photodynamic inactivation of *Streptococcus mutans* by curcumin in combination with EDTA. *Dent. Mater.* 37 (1), e1–e14.
- Pal, M., Shuramo, M.Y., Shiferawu, F., Parmar, B.C., 2022. Listeriosis: an emerging foodborne disease of public health concern. *J. Adv. Microsc. Res.* 3 (2), 29–33.
- Palacios, A., Otto, M., Flaherty, E., Boyle, M.M., Malec, L., Holloman, K., Low, M., Wellman, A., Newhart, C., Gollarza, L., 2022. Multistate outbreak of *Listeria monocytogenes* infections linked to fresh, soft hispanic-style cheese—United States, 2021. *MMWR (Morb. Mortal. Wkly. Rep.)* 71 (21), 709.
- Park, M.-Y., Kang, D.-H., 2021. Antibacterial Activity of Caffeic Acid Combined with Ultraviolet-A Light against *Escherichia coli* O157: H7, *Salmonella* Typhimurium and *Listeria Monocytogenes*. *Applied and environmental microbiology*. AEM. 00631-00621.
- Park, S.-H., Kang, D.-H., 2017. Influence of surface properties of produce and food contact surfaces on the efficacy of chlorine dioxide gas for the inactivation of foodborne pathogens. *Food Control* 81, 88–95.
- Peng, L., Wang, B., Ren, P., 2005. Reduction of MTT by flavonoids in the absence of cells. *Colloids Surf. B Biointerfaces* 45 (2), 108–111.
- Penha, C.B., Bonin, E., da Silva, A.F., Hioka, N., Zanqueta, É.B., Nakamura, T.U., de Abreu Filho, B.A., Campanerut-Sá, P.A.Z., Mikcha, J.M.G., 2017. Photodynamic inactivation of foodborne and food spoilage bacteria by curcumin. *LWT—Food Sci. Technol.* 76, 198–202.
- Priya, E.S., Selvakumar, K., Bavithra, S., Elumalai, P., Arunkumar, R., Singh, P.R., Mercy, A.B., Arunakaran, J., 2014. Anti-cancer activity of quercetin in neuroblastoma: an in vitro approach. *Neurol. Sci.* 35 (2), 163–170.
- Riddles, P.W., Blakeley, R.L., Zerner, B., 1979. Ellman's reagent: 5, 5'-dithiobis (2-nitrobenzoic acid)—a reexamination. *Anal. Biochem.* 94 (1), 75–81.
- Sebastianski, M., Bridger, N.A., Featherstone, R.M., Robinson, J.L., 2022. Disease outbreaks linked to pasteurized and unpasteurized dairy products in Canada and the United States: a systematic review. *Can. J. Public Health* 1–10.
- Sengupta, B., Sengupta, P.K., 2002. The interaction of quercetin with human serum albumin: a fluorescence spectroscopic study. *Biochem. Biophys. Res. Commun.* 299 (3), 400–403.
- Sheng, L., Li, X., Wang, L., 2022. Photodynamic inactivation in food systems: a review of its application, mechanisms, and future perspective. *Trends Food Sci. Technol.* 124, 167–181.
- Sheng, L., Zhu, M.J., 2021. Practical in-storage interventions to control foodborne pathogens on fresh produce. In: *Comprehensive Reviews in Food Science and Food Safety*.
- Shi, H., Zhang, R., Lan, L., Chen, Z., Kan, J., 2019. Zinc mediates resuscitation of lactic acid-injured *Escherichia coli* by relieving oxidative stress. *J. Appl. Microbiol.* 127 (6), 1741–1750.

- Silva, A.F., Borges, A., Giaouris, E., Graton Mikcha, J.M., Simões, M., 2018. Photodynamic inactivation as an emergent strategy against foodborne pathogenic bacteria in planktonic and sessile states. *Crit. Rev. Microbiol.* 44 (6), 667–684.
- Stiefel, P., Schmidt-Emrich, S., Maniura-Weber, K., Ren, Q., 2015. Critical aspects of using bacterial cell viability assays with the fluorophores SYTO9 and propidium iodide. *BMC Microbiol.* 15 (1), 1–9.
- Sutherland, M.W., Learmonth, B.A., 1997. The tetrazolium dyes MTS and XTT provide new quantitative assays for superoxide and superoxide dismutase. *Free Radic. Res.* 27 (3), 283–289.
- Temba, B.A., Fletcher, M.T., Fox, G.P., Harvey, J.J., Sultanbawa, Y., 2016. Inactivation of *Aspergillus flavus* spores by curcumin-mediated photosensitization. *Food Control* 59, 708–713.
- Treacy, J., Jenkins, C., Paranthaman, K., Jorgensen, F., Mueller-Doblies, D., Anjum, M., Kaindama, L., Hartman, H., Kirchner, M., Carson, T., 2019. Outbreak of Shiga toxin-producing *Escherichia coli* O157: H7 linked to raw drinking milk resolved by rapid application of advanced pathogen characterisation methods, England, August to October 2017. *Euro Surveill.* 24 (16), 1800191.
- Ukeda, H., Maeda, S., Ishii, T., Sawamura, M., 1997. Spectrophotometric assay for superoxide dismutase based on tetrazolium salt 3'-(1-[(phenylamino)-carbonyl]-3,4-tetrazolium)-bis (4-methoxy-6-nitro) benzenesulfonic acid hydrate reduction by xanthine-xanthine oxidase. *Anal. Biochem.* 251 (2), 206–209.
- Wang, Q., de Oliveira, E.F., Alborzi, S., Bastarrachea, L.J., Tikekar, R.V., 2017. On mechanism behind UV-A light enhanced antibacterial activity of gallic acid and propyl gallate against *Escherichia coli* O157: H7. *Sci. Rep.* 7 (1), 1–11.
- Wang, S., Yu, H., Wickliffe, J.K., 2011. Limitation of the MTT and XTT assays for measuring cell viability due to superoxide formation induced by nano-scale TiO₂. *Toxicol. Vitro* 25 (8), 2147–2151.
- Wu, J., Mou, H., Xue, C., Leung, A.W., Xu, C., Tang, Q.-J., 2016. Photodynamic effect of curcumin on *Vibrio parahaemolyticus*. *Photodiagnosis Photodyn. Ther.* 15, 34–39.
- Yujia, X., Wang, J., Li, Z., Luan, Y., Li, M., Peng, X., Xiao, S., Zhang, S., 2022. Damage prevention effect of milk-derived peptides on UVB irradiated human foreskin fibroblasts and regulation of photoaging related indicators. *Food Res. Int.* 161, 111798.
- Zhang, Y.-M., Zhang, Z.-Y., Wang, R.-X., 2020. Protective mechanisms of quercetin against myocardial ischemia reperfusion injury. *Front. Physiol.* 11, 956.
- Zhang, Y., Yang, C., Yang, D., Shao, Z., Hu, Y., Chen, J., Yuwen, L., Weng, L., Luo, Z., Wang, L., 2018. Reduction of graphene oxide quantum dots to enhance the yield of reactive oxygen species for photodynamic therapy. *Phys. Chem. Chem. Phys.* 20 (25), 17262–17267.
- Zhang, Z., Qin, J., Wang, Z., Chen, F., Liao, X., Hu, X., Dong, L., 2022. Sodium copper chlorophyll mediated photodynamic treatment inactivates *Escherichia coli* via oxidative damage. *Food Res. Int.*, 111472